PHYSICAL REVIEW D **93,** 065018 (2016)

Gauged multisoliton baby Skyrme model

A. Samoilenka[1] and Ya. Shnir[1,2]

[1]*Department of Theoretical Physics and Astrophysics Belarusian State University, Minsk 220004, Belarus*
[2]*Bogoliubov Laboratory for Theoretical Physics, Joint Institute for Nuclear Research, Dubna 141980, Moscow Region, Russia*

(Received 26 December 2015; published 7 March 2016)

We present a study of $U(1)$ gauged modification of the $2+1$-dimensional planar Skyrme model with a particular choice of the symmetry breaking potential term which combines a short-range repulsion and a long-range attraction. In the absence of the gauge interaction, the multisolitons of the model are aloof, as they consist of the individual constituents which are well separated. A peculiar feature of the model is that there are usually several different stable static multisoliton solutions of rather similar energy in a topological sector of given degree. We investigate the pattern of the solutions and find new previously unknown local minima. It is shown that coupling of the aloof planar multi-Skyrmions to the magnetic field strongly affects the pattern of interaction between the constituents. We analyze the dependency of the structure of the solutions, their energies, and magnetic fluxes on the strength of the gauge coupling. It is found that, generically, in the strong coupling limit, the coupling to the gauge field results in effective recovery of the rotational invariance of the configuration.

DOI: 10.1103/PhysRevD.93.065018

I. INTRODUCTION

The study of topological solitons in field theory can be traced back to the seminal paper by Skyrme [1] where the $SU(2)$-valued nonlinear model for atomic nuclei was suggested. The Skyrme model can be derived from the expansion of the QCD low-energy effective Lagrangian in the large N_c limit [2], then the topological charge of the multisoliton configuration is set into correspondence to the physical baryon number. Further, under certain assumptions, the semiclassical quantization of rotations and isorotations of the Skyrmions allows us to get a good approximation to the isospinning nuclei and describe the corresponding excitations which are associated with pions [3,4]. However, the Skyrme model has limited success, as there are several problems with description of the nuclear masses since the interaction energy of the Skyrmions is much higher than the corresponding experimental data for nuclei. Recent experimental observation of the heavy pentaquarks [5], which could be considered as a sort of baryon-meson bound state [6], also cannot be explained in the conventional Skyrme model with the usual pion mass term.

Several modifications of the Skyrme model in $3+1$ dimensions were suggested recently [7–10], mostly related with modification of the potential of the model. Furthermore, the contribution of the Coulomb electromagnetic energy is necessary to get a good agreement between the binding energies of the heavy nuclei and the predictions of the reduced BPS Skyrme model [7]. Therefore, it is physically natural to extend the model by gauging it to describe various electromagnetic processes of nucleons.

The $U(1)$ gauged Skyrme model was originally proposed in [11]; the axially symmetric gauged Skyrmions were later considered in [12,13]. It was noticed that the gauging of a $U(1)$ subgroup may stabilize the solitons even if the Skyrme term is dropped [14]; furthermore, in the gauged Skyrme model, the topological energy bound becomes saturated.

The planar reduction of the nonlinear sigma model is known as the baby Skyrme model [15,16]. This $(2+1)$-dimensional simplified model resembles the basic properties of the genuine Skyrme model in many aspects. Furthermore, the baby Skyrme model has a number of applications on its own, e.g., in condensed matter physics where Skyrmion configurations were observed experimentally [17], in the description of the topological quantum Hall effect [18,19], or in brane cosmology where the solitons of the model induce warped compactification of the two-dimensional extra space [20]. Also, it was found that the restricted baby Skyrme model in $2+1$ dimensions has BPS soliton solutions saturating the topological bound [21].

A peculiar feature of the planar Skyrme model is related to the particular choice of the potential term which is necessary to stabilize the solitons.[1] In low-dimensional systems, the effect of this term becomes more significant than in the original Skyrme model; for example, there are different choices of the potential related with various kinds

[1]Note that a special choice of the parameters of the baby Skyrme model allows to evade the potential term and construct static soliton solutions in the reduced model [22]; however, dynamical properties of these special configurations are still unknown.

of symmetry breaking [23–26]. In particular, a suitable choice for the potential term allows us to separate the individual constituents of the planar Skyrmions, each of them being associated with a fractional part of the topological charge of the configuration [25]. Another possibility is to combine a short-range repulsion and a long-range attraction between the solitons [26,27]. Then the multisoliton configuration consists of aloof constituents.

Clearly, coupling the model to the electromagnetic field yields another possible channel of interaction between the solitons. Analysis of the gauged baby Skyrmions [28] reveals very interesting features of the corresponding solutions which carry a nonquantized nontopological magnetic flux. Further, if the Chern-Simons term is additionally included in the Lagrangian, the planar Skyrmions become electrically charged [29]. Recently, the properties of the soliton configurations in the gauged BPS baby Skyrme model were investigated [30]. An interesting observation is that, in the strong coupling limit, the magnetic flux becomes quantized though there is no topological reason for that [28,31].

The aim of this paper is to discuss the structure of the soliton solutions of the gauged aloof baby Skyrme-Maxwell system with a rotationally invariant potential term analogous to that used in [26,27]. Our calculations are performed for multisoliton solutions up to charge 10. We study numerically the dependence of masses of these configurations and the corresponding magnetic fluxes on the gauge coupling constant, both in the perturbative limit and in the strong coupling limit without any restrictions of symmetry.

II. THE MODEL

We consider a gauged version of the $O(3)$ σ model with the Skyrme term in $2+1$ dimensions [16] with a Lagrangian

$$\mathcal{L} = -\frac{1}{4}F_{\mu\nu}F^{\mu\nu} + \frac{1}{2}D_\mu\phi^a D^\mu\phi^a - \frac{1}{4}(\varepsilon_{abc}\phi^a D_\mu\phi^b D_\nu\phi^c)^2 - V. \quad (1)$$

Here ϕ^a denotes a triplet of scalar fields, which is constrained to the surface of a sphere of unit radius $\phi^a\phi^a = 1$. We introduce the usual Maxwell term with the field strength tensor defined as $F_{\mu\nu} = \partial_\mu A_\nu - \partial_\nu A_\mu$. Clearly, the scaling dimensions of this term and the Skyrme term, which is quartic in derivatives, are identical.

The coupling of the scalar field to the $U(1)$ gauge field A_μ is given by the covariant derivative [14,28,32]

$$D_\mu\phi^a = \partial_\mu\phi^a + gA_\mu\varepsilon_{abc}\phi^b\phi^c_\infty, \quad (2)$$

where g is the gauge coupling constant. The localized field configuration has finite energy if $D_\mu\phi^a \to 0$, $F_{\mu\nu} \to 0$ and $V \to 0$ as $r \to \infty$.

The topological restriction on the field ϕ^a is that it approaches its vacuum value at spacial boundary, i.e. $\phi^a_\infty = (0,0,1)$. This allows a one-point compactification of the domain space $\mathbb{R}^2$ to $\mathbb{S}^2$ and the field of the finite energy solutions of the model is a map $\boldsymbol{\phi}$: $\mathbb{R}^2 \to \mathbb{S}^2$ which belongs to an equivalence class characterized by the topological charge $Q = \pi_2(\mathbb{S}^2) = \mathbb{Z}$. Explicitly,

$$Q = -\frac{1}{4\pi}\varepsilon_{abc}\int \phi^a\partial_x\phi^b\partial_y\phi^c dxdy. \quad (3)$$

A special feature of the solutions of the planar Skyrme model is that their structure strongly depends on the particular form of the potential term V. The most common choice is the so-called "old potential" [16]

$$V = \mu^2[1-\phi_3], \quad (4)$$

which is an analogue of the standard pion mass term in the $(3+1)$-dimensional Skyrme model. The symmetry is broken via the potential to $SO(2)$, and there is a unique vacuum $\boldsymbol{\phi}_\infty = (0,0,1)$. The corresponding solitons of degree $Q = 1$, 2 are axially symmetric [16]; however, the rotational symmetry of the configurations of higher degree becomes broken [33].

In the model with double vacuum potential (or "easy-axis" potential) [15,34],

$$V = \mu^2(1-\phi_3^2), \quad (5)$$

the multisoliton solutions are rotationally invariant over entire range of values of the mass parameter μ. The most general case of the one-parametric potential,

$$V = \mu^2(1-\phi_3)^s, \quad (6)$$

with $0 < s \leq 4$ was considered in [24]. Since the "old" potential (4) corresponds to the attractive force acting between the solitons, while the "holomorphic" potential $V = \mu^2(1-\phi_3)^4$ is repulsive [35,36], the parameter s in the potential (6) is responsible for the balance of the repulsive and attractive interaction between the Skyrmions. Further, one can consider the linear combination of the "old" and "holomorphic" potentials [26,27],

$$V = \mu^2[\lambda(1-\phi_3) + (1-\lambda)(1-\phi_3)^4], \quad \lambda \in [0,1], \quad (7)$$

which corresponds to a short-range repulsion and a long-range attraction between the solitons. Following [26,27], we restrict our consideration to the case $\lambda = 0.5$.

The resulting multisoliton configuration is no longer rotationally invariant—each constituent of unit charge is clearly separated from the other, and they form a cluster structure. Further, in the absence of the gauge interaction, there are usually several different static multisoliton solutions of rather similar energy in a topological sector of

given degree [26]. Note that this feature is like the Hopfion solutions of the Faddeev-Skyrme model [37]. Indeed, the structure of both models looks similar—the corresponding Lagrangian (1) includes the usual sigma model term, the Skyrme term, which is quartic in derivatives of the field, and the potential term. Further, the field of the Faddeev-Skyrme model in three spacial dimensions is also a three-component unit vector restricted to the unit sphere S^2. However, the domain space of the latter model is the compactified three-dimensional sphere S^3, and the Hopfion solutions are classified by the linking number associated with the homotopy group $\pi_3(S^2) = \mathbb{Z}$. Thus, in some sense, the baby Skyrme model can be considered as a planar reduction of the Faddeev-Skyrme model [38].

In $2+1$ dimensions, the electric field of configuration is vanishing everywhere [28], and we can consider a purely magnetic field generated by the Maxwell potential,

$$A_0 = A_y = 0, \qquad A_x = A(x,y), \tag{8}$$

where the gauge fixing condition is used to exclude the A_y component of the vector potential. Thus, the magnetic field is orthogonal to the x-y plane: $B = B_z = -\partial_y A_x$. Note we do not use here the rotationally invariant parametrization of the fields where the gauge-fixing condition $A_r = 0$ is imposed [15,16,34].

The complete set of the field equations, which follows from the variation of the action of the baby Skyrme-Maxwell model (1), can be solved when we impose the boundary conditions. As usual, they follow from the regularity on the boundaries and symmetry requirements as well as the condition of finiteness of the energy and topology. In particular, we have to take into account that the magnetic field is vanishing on the spacial asymptotic. Explicitly, on the spacial boundary, we impose

$$\phi_1\Big|_{r\to\infty} \to 0, \qquad \phi_2\Big|_{r\to\infty} \to 0, \qquad \phi_3\Big|_{r\to\infty} \to 1,$$
$$\partial_y A\Big|_{r\to\infty} \to 0. \tag{9}$$

Here $r = \sqrt{x^2+y^2}$ is the usual radial variable.

As an initial guess for further computation, we used various combinations of single solitons with preassigned phases and positions. These field configurations can be constructed via the usual parametrization of the unit scalar triplet ϕ^a in terms of the complex field W via the stereographic projection:

$$W = \frac{\phi_1 + i\phi_2}{1-\phi_3}. \tag{10}$$

Let $W_i(z)$, $z = x+iy$, be the field of a single Skyrmion of degree one with an arbitrary position and phase, then the function $\frac{1}{W} = \sum \frac{1}{W_i}$, $i = 1, 2, ..Q$ allows us to obtain the field of the multisoliton configuration of degree Q with various relative phases and separations. For example, the function

$$W(z) = \frac{4}{(z-2)^{-1} - (z-1)^{-1} + z^{-1} - (z+1)^{-1} + (z+2)^{-1}} \tag{11}$$

yields the input configuration in the sector of degree $Q = 5$, which represents the chain of baby Skyrmions with opposite relative orientations and separation between the constituents $d = 1$.

III. NUMERICAL RESULTS

In this section, we outline our method for calculating the multisoliton solutions of the gauged baby Skyrme model. The numerical calculations are mainly performed on a equidistant square grid, typically containing 160^2 lattice points and with a lattice spacing $dx = 0.15$ To check our results for consistency, we also considered the lattice spacings $dx = 0.1$, 0.2.

To construct multisoliton solutions of the model (1), we minimize the corresponding rescaled energy functional of the static configuration,

$$E = \int \left\{ \frac{1}{2}B^2 + \frac{1}{2} D_i\phi^a \cdot D_i\phi^a + \frac{1}{4}(\varepsilon_{abc}\phi^a D_i\phi^b D_j\phi^c)^2 + V \right\} dxdy, \tag{12}$$

with the aloof baby Skyrmions potential (7). The gauge coupling g is a parameter, with each of our simulations beginning at $g = 0$ with a fixed value of μ and λ, then we proceed by making small increments in g. For comparative consistency with [26], in most of our calculations we choose $\mu^2 = 0.1$ and $\lambda = 0.5$.

The numerical algorithm employed was similar to that used in [39]. Well-chosen initial configurations of given degree were evolved using the Metropolis method to minimize the energy functional (12). In our numerical calculations, we introduce an additional Lagrange multiplier to constrain the field to the surface of the unit sphere. Simulations were considered to have converged to local minima if the quantity $-\frac{1}{E}\frac{dE}{dt}$ becomes less than 10^{-3}, where t is the time of computation in minutes. We also verify that the evaluated topological charge of the configuration is in agreement with the input integer value.

Another check of the correctness of our results was performed by finding corresponding solutions of the Euler-Lagrange equations which follow from the Lagrangian (1) subject to a set of boundary conditions (9). The relative errors of the solutions we found implementing the

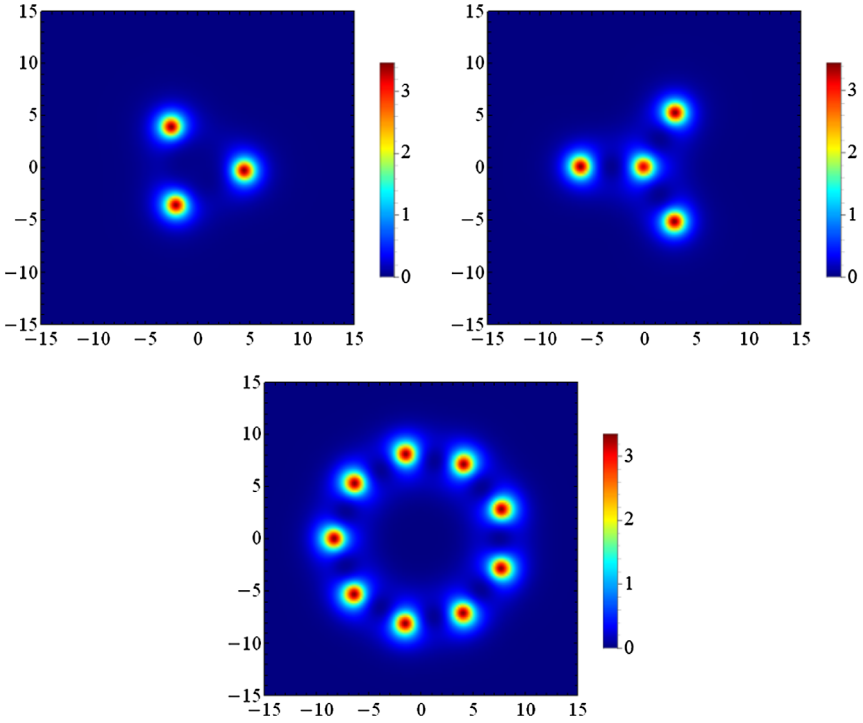

FIG. 1. Contour energy density plots of the $3D_3$, $4D_3$ and $9D_9$ of planar Skyrmions in the model (1) at $g = 0$.

Newton-Raphson fourth-order finite difference method are of order of 10^{-4} or smaller.

First, we recover the usual $Q = 1$ solution. Its energy for $g = 0$ is $E_1 = 20.25$; this is within 0.1% of the previously known result [26]. This similarity is another nice validation of our numerical algorithm.

Since there are a variety of configurations of planar aloof Skyrmions, in order to distinguish these multisolitons, we are using the following notation: QD_n where Q is the topological charge of the planar configuration or its building block and D_n is the dihedral group of corresponding symmetry. For example, in the sector of degree four, we have found the $4D_4$ (which is the global minimum at $g = 0$), $4D_3$, and $4D_2$ solutions.

Note that among solutions we constructed using the rational map input (10), there are new configurations, which were not considered in [26] since they represent local minima. In Fig. 1, we exhibited the energy density plots of some of these new solutions, $3D_3$, $4D_3$, and $9D_9$, respectively.

Constructing these configurations, we vary relative orientation χ of the constituents in the internal space. Indeed, the total potential of interaction between two neighboring baby Skyrmions is proportional to $\cos\chi$ [16] and repulsive if the solitons are in phase ($\chi = 0$). The most attractive channel corresponds to opposite orientations of the solitons, $\chi = \pi$.

However, the interaction energy is still negative for the solitons which are not completely out of phase. If the number of constituents is even, they always form pairs with opposite relative orientation; however, for a system of N solitons, where N is an odd number, another possibility exists. The solitons may form a circular necklace where each of N baby Skyrmions is rotated by angle $(1 - \frac{1}{N})\pi$ with respect to its neighbor. Hence, in this case, we considered composite solutions with N soliton species, not only binary species like in [26]. Thus, for odd N the total angle of internal rotation along the ring is $\pi(N - 1) = 2\pi k$, where k is integer. Particular examples of this type, the $3D_3$ and $9D_9$ solutions, are displayed in Fig. 1. Clearly, configurations of that type represent local minima.

Another interesting example of configuration, which also was not discussed in [26], is the "tristar" configurations $4D_3$ of degree four. Here the relative phase of the three solitons with respect to the central constituent is π; however, with respect to each other, they are in phase, $\chi = 0$. Thus, the central component provides strong attraction to the outer solitons binding the configuration together.

As the gauge coupling increases from zero, the energy of the gauged aloof Skyrmions decreases since the magnetic flux is formed. Now each individual Skyrmion is coupled to a magnetic flux, and the electromagnetic interaction modifies the usual pattern of the scalar interaction of constituents. Effectively, the asymptotic field of the gauged soliton represents a triplet of dipoles, two scalar dipole moments are associated with the asymptotic form of the scalar fields ϕ_1, ϕ_2 in the x-y plane, and the third magnetic dipole is orthogonal to this plane [28].

Note that, effectively, using the Maxwell equation $\nabla \times \vec{B} = \vec{j}$, one can set the magnetic field into

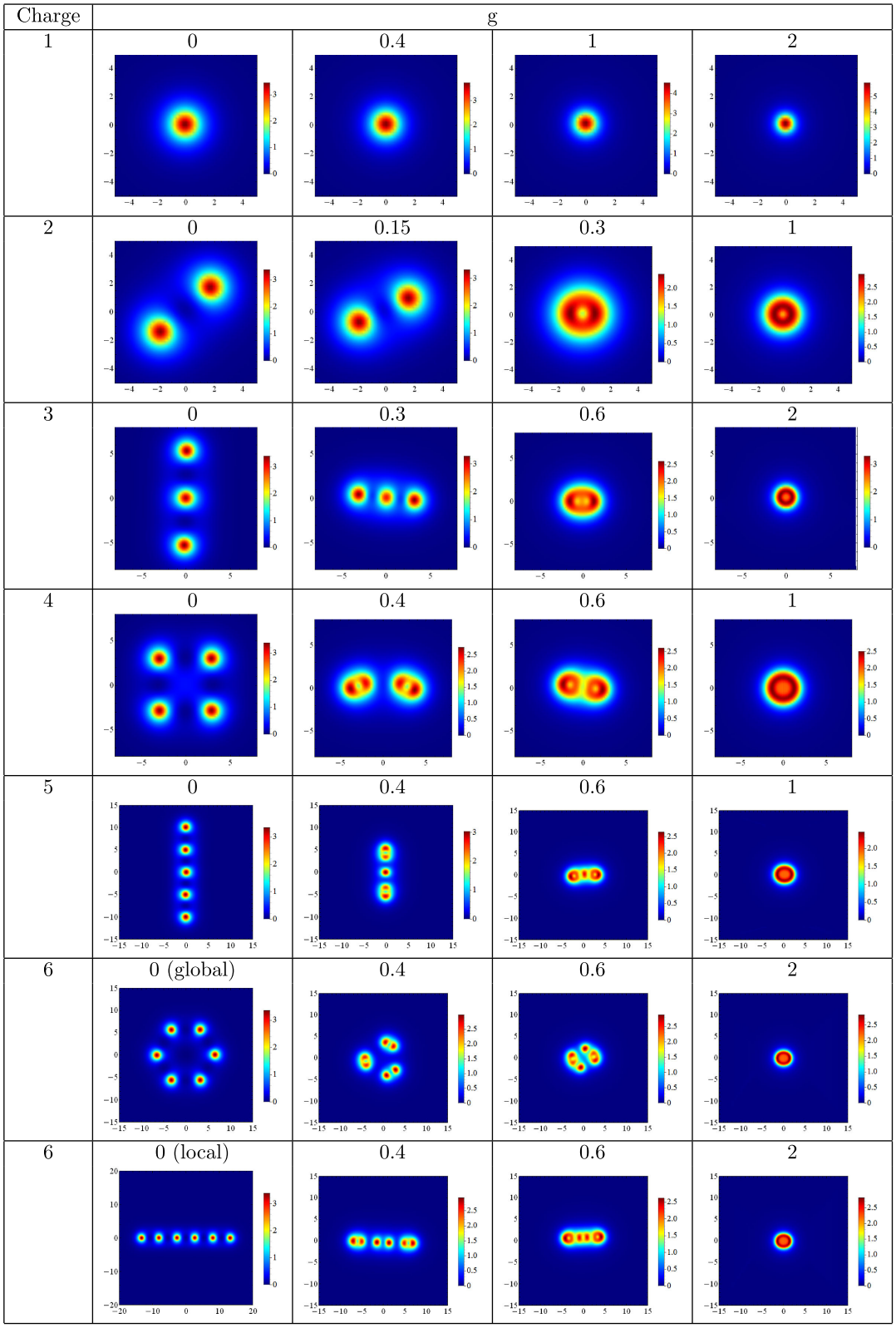

FIG. 2a. Energy density plots for $1 \leq Q \leq 6$ gauged planar Skyrmions in the model (1) at some set of values of $g \in [0, 2]$ and $\mu^2 = 0.1$ and $\lambda = 0.5$.

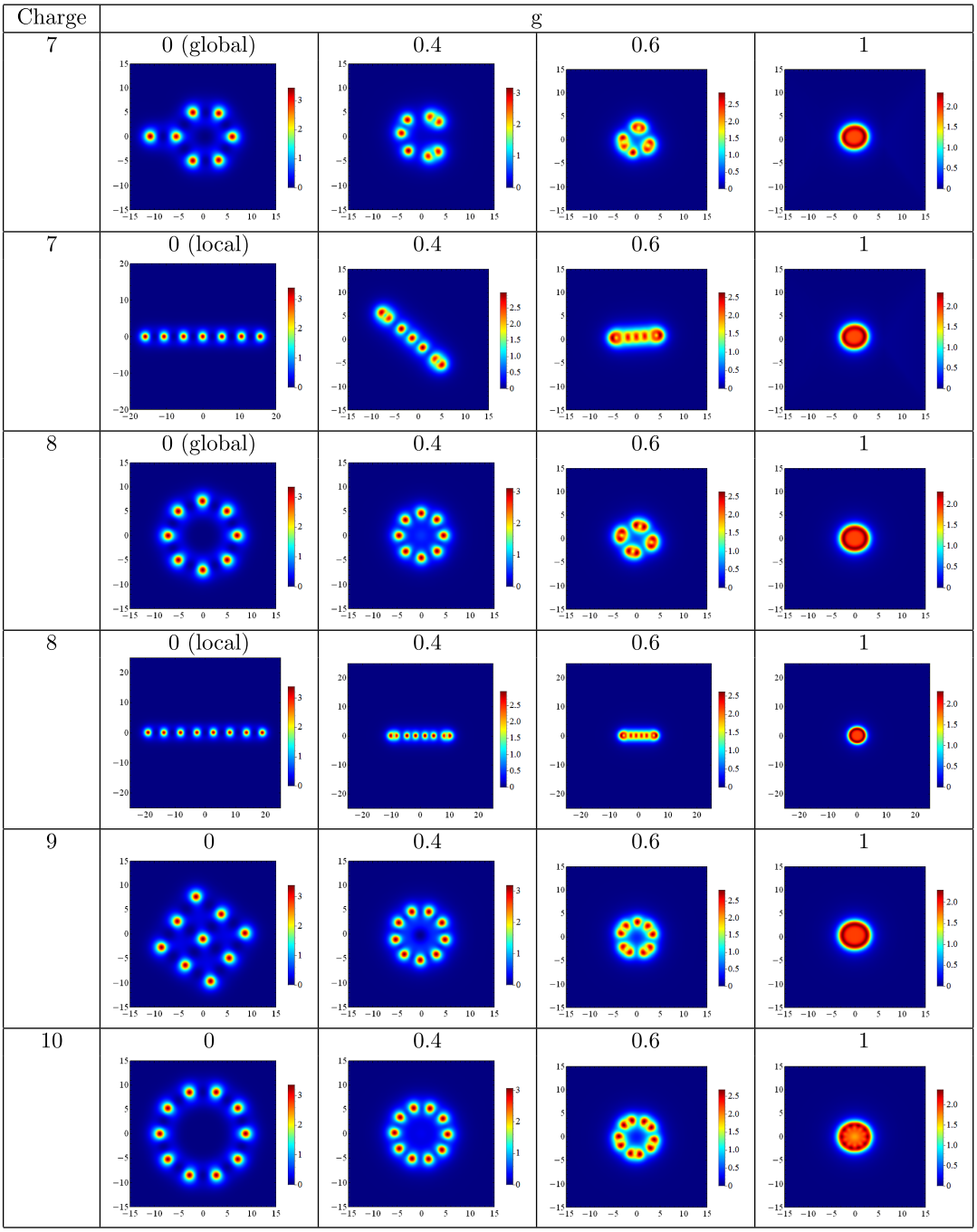

FIG. 2b. Energy density plots for $7 \leq Q \leq 10$ gauged planar Skyrmions in the model (1) at some set of values of $g \in [0; 2]$ and $\mu^2 = 0.1$ and $\lambda = 0.5$.

correspondence with an effective circular electric current j_ν. On the other hand, the term $\sim g^2 A^2 \phi^2$ in the total Hamiltonian of the system effectively contributes to the mass of the scalar field; thus, the Yukawa interaction between the gauged baby Skyrmions becomes stronger.

In Fig. 2, we exhibited the contour energy density plots of the gauged baby Skyrmions in the model (1) for $1 \leq Q \leq 10$ at some set of values of the gauge coupling $g \in [0.2]$. First, we observe that for relatively small values of the coupling constant g, two neighboring solitons with opposite orientations form pairs in accordance with the binary species model [26].

Let us consider a few particular configurations. In Fig. 3, left plot, we have plotted the dependency of the energy of the static gauged baby Skyrmion of unit charge and the chains $2D_2$, $5D_2$, $8D_2$ as functions of g. In the right plot, we also displayed the soliton's binding energy $\Delta E = QE_1 - E$ as a function of the gauge

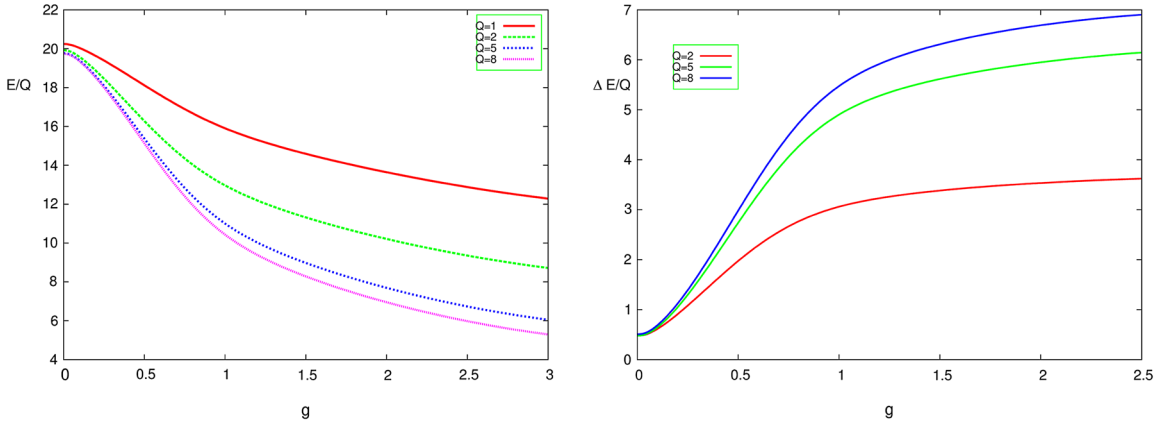

FIG. 3. The normalized energy per charge E of the $Q = 1, 2, 5, 8$ chains of gauged baby Skyrmions (left plot), and the corresponding binding energy per charge (right plot) as a function of the coupling constant g at $\mu^2 = 0.1$ and $\lambda = 0.5$.

coupling. Here E_1 is the energy of the one-soliton configuration at the corresponding value of the gauge coupling g, and we used the normalized units of energy per unit charge. From these plots, it is clear that the energy of the configurations decreases as the gauge coupling becomes stronger while the binding energy is increasing. Thus, the balance between the repulsive and attractive forces in the ungauged model with the potential (7) is shifted towards the attraction and, as coupling becomes strong enough, the rotational invariance of the multisoliton configuration is restored. Further increasing of the gauge coupling makes the solitons' width increasingly localized.

Note that as the coupling remains smaller than one, the electromagnetic energy E_{em} is increasing; however, in the strong coupling limit, its contribution begins to decrease as g continues to grow, as seen in Fig. 4, left plot.

We can understand this effect if we note that the conventional rescaling of the potential $A_\mu \to gA_\mu$ leads to $F^2_{\mu\nu} \to \frac{1}{g^2} F^2_{\mu\nu}$. Thus, the very large gauge coupling effectively removes the Maxwell term leaving the limiting configuration of the gauged planar Skyrmions coupled to a circular magnetic vortex of constant flux. Apparently, in such a limit, the strong coupling with a vortex yields an effective potential term which supplements the potential (7).

Let us note that the particular choice of the parameters of the aloof potential (7) is related with the condition of balance between a short-range repulsion and a long-range attraction, decreasing of the parameter λ increases the repulsive component. Coupling to magnetic field modifies the structure of interactions, as the coupling g increases, the attractive part of interaction becomes stronger. As a result, we can approach the limit $\lambda \to 0$ providing the gauge coupling is nonvanishing. In such a limit, variation of the coupling g allows us to manipulate the attractive part of interaction between the Skyrmions. Further, at some critical value of the gauge coupling there is a transition from the aloof structure of the multisolitons to the rotationally invariant configuration, for example in the sector of degree $Q = 2$ it happens as $g = 0.45$ and $\lambda = 0$.

Thus, the configurations carry total magnetic flux $\Phi = \int d^2x B$, which is in general, nonquantized. The flux of the gauged baby Skyrmions is associated with the position of the solitons and is orthogonal to the $x-y$ plane [28]. In the usual model with rotationally invariant

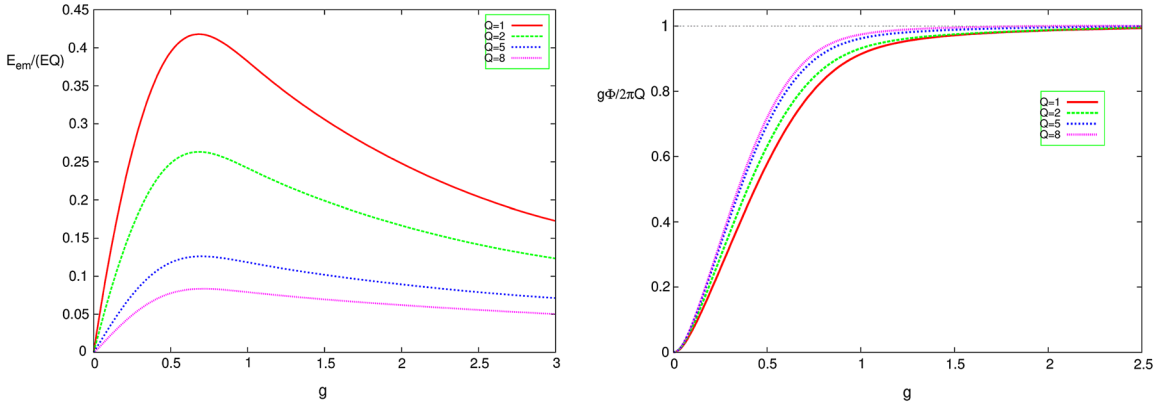

FIG. 4. The ratio per charge of the magnetic energy E_{em} to the total energy E of the $Q = 1, 2, 5, 8$ chains of gauged baby Skyrmions (left plot), and the magnetic flux through the x-y plane (right plot) as a function of the coupling constant g at $\mu^2 = 0.1$ and $\lambda = 0.5$.

potential (5), or in the strong coupling limit of the gauge model (1), there is a single magnetic flux through the center of the soliton, in the aloof system, where rotational invariance becomes violated and each unit charge constituent of the multisoliton configuration is coupled to a flux.

An interesting observation is that, as the gauge coupling becomes stronger, the magnetic flux of the degree Q baby Skyrmions grows from 0 to $2\pi Q/g$; i.e., in the strong coupling regime, the magnetic flux is quantized though there is no topological reason for it [28]. Indeed, in Fig. 4, right plot, we display the results of our numerical calculations of the integrated magnetic field of the gauged planar Skyrmion through the x-y plane. In the limit $g = 0$, the magnetic flux is vanishing; in the weak coupling regime $0 \leq g \lesssim \mu$, the fluxes are attached to the individual partons of the multisoliton configuration.

As gauge coupling increases further, the radius of the each vortex is getting smaller and the magnitude of the magnetic field increases significantly. For $g > 1$, the flux tends to be quantized in units of $2\pi/g$ and the configuration becomes rotationally invariant. The energy density distribution in the strong coupling limit is localized near the center of the configuration approaching a singular string-like distribution in the limit $g \to \infty$ [28].

IV. CONCLUSION

The main purpose of this work is to present a new type of gauged soliton in the planar Skyrme-Maxwell theory. In the model with aloof potential (7), the individual solitons are composed of the constituents with unit topological charge. A peculiar feature of the model is that, similar to the solutions of the Faddeev-Skyrme model, a number of local energy minima of various types exists in each topological sector. Coupling of the solitons to the gauge sector yields additional attractive interaction which modifies the structure of configurations of given degree. It has been shown that the rotational invariance of the multisoliton configuration is restored in the strong coupling regime.

Similar to the corresponding solutions in the gauged Skyrme model and Faddeev-Skyrme model [40], the planar configurations are topologically stable, and in the weak coupling regime they carry a nonquantized magnetic flux which is orthogonal to the x-y plane and penetrates the Skyrmion. In the strong coupling limit, the total magnetic flux, associated with the partons, becomes quantized in units of topological charge.

We confirm that the mass of the static configuration decreases when the electromagnetic coupling constant is increased; thus, a baby Skyrmion can lower its mass by interacting with the electromagnetic field. Also, when g is increasing, the binding energy of the solitons increases.

Finally, note that the planar Skyrmions appear as quasiparticles in various systems; in particular, they are natural objects in the description of the integer quantum Hall effect [19]. The vortices coupled to the planar Skyrmion constituents may appear in multicomponent superconductors [41]; thus, as avenues for further research, it would be interesting to extend the solutions in this work to the effective condensed matter systems where the scalar field of the model is the order parameter. In such a context, there is a phase transition related with rotational symmetry breaking at some critical value of the gauge coupling and separation of the individual solitons. The phase with unbroken symmetry corresponds to the strong coupling limit, while the symmetry becomes broken in the weak coupling limit; thus, this situation resembles the usual pattern of the second-order phase transition in superconductors.

Another interesting possibility is to consider the gauged baby Skyrme model with aloof potential and Chern-Simons term [29] without restrictions of symmetry, which would allow us to include the electric field in our consideration.

ACKNOWLEDGMENTS

We thank Igor Bogolubsky, Derek Harland, Martin Speight, and Andrzej Wereszczyński for useful discussions and valuable comments. This work is supported in part by the A. von Humboldt Foundation in the framework of the its linkage program. Some of the work of Y. S. was supported by the Russian Foundation for Basic Research (Grant No. 16-52-12012). Most numerical calculations were performed on the HybriLIT cluster at the JINR, Dubna.

[1] T. H. R. Skyrme, Proc. R. Soc. A **260**, 127 (1961).
[2] E. Witten, Nucl. Phys. **B223**, 422 (1983); **B223**, 433 (1983).
[3] G. S. Adkins, C. R. Nappi, and E. Witten, Nucl. Phys. **B228**, 552 (1983).
[4] *The Multifaceted Skyrmion*, edited by G. E. Brown and M. Rho (World Scientific, Singapore, 2010).
[5] R. Aaij *et al.* (LHCb Collaboration), Phys. Rev. Lett. **115**, 072001 (2015).
[6] M. Karliner and J. L. Rosner, Phys. Rev. Lett. **115**, 122001 (2015).
[7] C. Adam, C. Naya, J. Sanchez-Guillen, and A. Wereszczynski, Phys. Rev. Lett. **111**, 232501 (2013).
[8] P. Sutcliffe, J. High Energy Phys. 04 (2011) 045.

[9] V. B. Kopeliovich, B. Piette, and W. J. Zakrzewski, Phys. Rev. D **73**, 014006 (2006).
[10] S. B. Gudnason and M. Nitta, Phys. Rev. D **91**, 085040 (2015).
[11] C. J. Callan Jr. and E. Witten, Nucl. Phys. **B239**, 161 (1984).
[12] B. M. A. G. Piette and D. H. Tchrakian, Phys. Rev. D **62**, 025020 (2000).
[13] E. Radu and D. H. Tchrakian, Phys. Lett. B **632**, 109 (2006).
[14] B. J. Schroers, Phys. Lett. B **356**, 291 (1995).
[15] A. A. Bogolubskaya and I. L. Bogolubsky, Phys. Lett. A **136**, 485 (1989); Lett. Math. Phys. **19**, 171 (1990).
[16] B. M. A. G. Piette, W. J. Zakrzewski, H. J. W. Mueller-Kirsten, and D. H. Tchrakian, Phys. Lett. B **320**, 294 (1994); B. M. A. G. Piette, B. J. Schroers, and W. J. Zakrzewski, Z. Phys. C **65**, 165 (1995).
[17] X. Z. Yu, Y. Onose, N. Kanazawa, J. H. Park, J. H. Han, Y. Matsui, N. Nagaosa, and Y. Tokura, Nature (London) **465**, 901 (2010).
[18] A. Neubauer, C. Pfleiderer, B. Binz, A. Rosch, R. Ritz, P. G. Niklowitz, and P. Böni, Phys. Rev. Lett. **102**, 186602 (2009).
[19] S. M. Girvin, The quantum Hall effect: Novel excitations and broken symmetries, in *Aspects topologiques de la physique en basse dimension. [Topological aspects of low dimensional systems]* (Springer, Berlin, 1999), p. 53.
[20] Y. Kodama, K. Kokubu, and N. Sawado, Phys. Rev. D **79**, 065024 (2009).
[21] C. Adam, T. Romanczukiewicz, J. Sanchez-Guillen, and A. Wereszczynski, Phys. Rev. D **81**, 085007 (2010).
[22] J. Ashcroft, M. Haberichter, and S. Krusch, Phys. Rev. D **91**, 105032 (2015).
[23] R. S. Ward, Nonlinearity **17**, 1033 (2004).
[24] I. Hen and M. Karliner, Nonlinearity **21**, 399 (2008).
[25] J. Jäykkä, J. M. Speight, and P. Sutcliffe, Proc. R. Soc. A **468**, 1085 (2012).
[26] P. Salmi and P. Sutcliffe, J. Phys. A **48**, 035401 (2015).
[27] P. Salmi and P. Sutcliffe, arXiv:1511.03482.
[28] J. Gladikowski, B. M. A. G. Piette, and B. J. Schroers, Phys. Rev. D **53**, 844 (1996).
[29] A. Yu. Loginov, JETP **118**, 217 (2014).
[30] C. Adam, T. Romanczukiewicz, J. Sanchez-Guillen, and A. Wereszczynski, J. High Energy Phys. 11 (2014) 095.
[31] Y. M. Shnir, Phys. Part. Nucl. Lett. **12**, 469 (2015).
[32] C. Adam, C. Naya, J. Sanchez-Guillen, and A. Wereszczynski, Phys. Rev. D **86**, 045010 (2012).
[33] B. M. A. G. Piette, B. J. Schroers, and W. J. Zakrzewski, Nucl. Phys. **B439**, 205 (1995).
[34] T. Weidig, Nonlinearity **12**, 1489 (1999).
[35] R. A. Leese, M. Peyrard, and W. J. Zakrzewski, Nonlinearity **3**, 773 (1990).
[36] P. Sutcliffe, Nonlinearity **4**, 1109 (1991).
[37] L. D. Faddeev, Quantization of Solitons, Princeton preprint IAS-75-QS70 (1975); L. D. Faddeev and A. Niemi, Nature (London) **387**, 58 (1997); Phys. Rev. Lett. **82**, 1624 (1999).
[38] M. Kobayashi and M. Nitta, Nucl. Phys. **B876**, 605 (2013).
[39] M. Hale, O. Schwindt, and T. Weidig, Phys. Rev. E **62**, 4333 (2000).
[40] Ya. Shnir and G. Zhilin, Phys. Rev. D **89**, 105010 (2014).
[41] E. Babaev, J. Jaykka, and J. M. Speight, Phys. Rev. Lett. **103**, 237002 (2009).